chain lengths. We therefore suggest that the face-centered cubic lattice model is the better lattice model for simulating the effects of concentration on chain dynamics.

The normal mode analysis suggests that the excluded volume constraint acts in a continuous manner at the length scales probed in this study. Since the chain lengths studied were short and only the first three normal modes were studied, this deserves further investigation. We also observed that the chain length dependence of the relaxation time increases with mode number. This effect can be explained in terms of the blob model.

Clearly these results are preliminary. Because of limited computer time only a limited number of chain lengths were studied. We feel that the basic results will be corroborated by studies on systems with longer chains. We also feel that the face-centered cubic lattice model is an excellent model for the study of a variety of problems in polymer melt dynamics.

**Acknowledgment** is made to the U.S. Department of Energy, Office of Basic Energy Sciences, Division of Materials Sciences, and to the donors of the Petroleum Research Fund, administered by the American Chemical Society, for partial support of this research. We thank the University of Tennessee Computer Center for their continuing support. We thank the Rohm and Haas Computer Applications Research Department for their assistance.

## References and Notes

(1) de Gennes, P.-G. *J. Chem. Phys.* **1971**, *55*, 572. de Gennes, P.-G. *Scaling Concepts in Polymer Physics*; Cornell University Press: Ithaca, NY, 1979.
(2) Graessley, W. W. *Adv. Polym. Sci.* **1982**, *47*, 67. de Gennes, P.-G.; Leger, L. *Ann. Rev. Phys. Chem.* **1982**, *33*, 49.
(3) Richter, D.; Baumgartner, A.; Binder, K.; Ewen, B.; Hayter, J. B. *Phys. Rev. Lett.* **1981**, *47*, 2994. Higgins, J. S.; Roots, J. E. *J. Chem. Soc., Faraday Trans. 2* **1985**, *81*, 757.
(4) Wheeler, L. M.; Lodge, T. P.; Hanley, B.; Tirrell, M. *Macromolecules* **1987**, *20*, 1120.
(5) Baumgartner, A. *Ann. Rev. Phys. Chem.* **1984**, *35*, 419.
(6) Kranbuehl, D. E.; Verdier, P. H. *Macromolecules* **1985**, *18*, 1638.
(7) Crabb, C. C.; Kovac, J. *Macromolecules* **1985**, *18*, 1430.
(8) Kolinski, A.; Skolnick, J.; Yaris, R. *J. Chem. Phys.* **1986**, *84*, 1922; **1987**, *86*, 7164; **1987**, *86*, 7174; **1987**, *86*, 1567.
(9) Kranbuehl, D. E.; Verdier, P. H. *Macromolecules* **1984**, *17*, 749.
(10) Downey, J. P.; Kovac, J. *Macromolecules* **1987**, *20*, 1357.
(11) Gurler, M. T.; Crabb, C. C.; Dahlin, D. M.; Kovac, J. *Macromolecules* **1983**, *16*, 398.
(12) Verdier, P. H.; Kranbuehl, D. E. *Macromolecules* **1987**, *20*, 1362.
(13) Stokely, C.; Crabb, C. C.; Kovac, J. *Macromolecules* **1986**, *19*, 860.
(14) Downey, J. P.; Crabb, C. C.; Kovac, J. *Macromolecules* **1986**, *19*, 2202.
(15) Verdier, P. H. *J. Chem. Phys.* **1966**, *45*, 2118.
(16) Hilhorst, H. J.; Deutch, J. M. *J. Chem. Phys.* **1975**, *63*, 5153.
(17) Verdier, P. H.; Stockmayer, W. H. *J. Chem. Phys.* **1962**, *36*, 227.
(18) Kranbuehl, D. E.; Verdier, P. H. *J. Chem. Phys.* **1979**, *71*, 2662.
(19) Naghizadeh, J.; Kovac, J. *Phys. Rev. B* **1986**, *34*, 1984.

# Distribution of Matrix Homopolymer in Block Copolymers of Spherical Morphology

**C. V. Berney,† Pao-Luo Cheng,‡ and R. E. Cohen*,†**

*Department of Chemical Engineering and Department of Materials Science and Engineering, Massachusetts Institute of Technology, Cambridge, Massachusetts 02139.*
*Received September 28, 1987; Revised Manuscript Received February 17, 1988*

ABSTRACT: Samples made by blending deuteriated polystyrene $S_d$ of three different molecular weights with a polystyrene–polybutadiene block copolymer SB were studied with small-angle scattering techniques using X-rays (SAXS) and neutrons (SANS). The SANS results were sensitive both to the amount of added homopolymer $S_d$ and to its chain length. Anomalously high SANS intensities and the absence of an intraparticle scattering maximum are consistent with the exclusion of added $S_d$ from the corona of the SB micelles, resulting in $S_d$ enrichment of the interstitial regions.

## Introduction

The study of block copolymers has proved to be a fertile area for the detailed elucidation of polymer interactions; it has been particularly fruitful in the production of information generated through the interplay between theoretical studies (see, for example, papers by Meier,[1] Helfand,[2] Leibler,[3-5] and Noolandi[6,7] and their co-workers) and experimental work, particularly small-angle scattering studies involving X-rays (SAXS) and neutrons (SANS).

One of the advantages of SANS over SAXS is the possibility of manipulating the contrast (in SANS, the nuclear scattering-length density) by selective deuteriation. This technique was exploited in previous studies[8,9] by synthesizing a polystyrene–polybutadiene diblock with the polybutadiene segment deuteriated ($SB_d$) to enhance the contrast between the spherical polybutadiene microdomains and the polystyrene matrix; the SANS signal was increased by a factor of 27, allowing detection of Debye–Scherrer powder peaks characteristic of cubic packing of the $B_d$ domains[8] and accurate assessment of sphere size and interfacial thickness for a number of samples of differing molecular weight.[9] In another experiment,[10] deuteriated polystyrene–polybutadiene diblocks $SB_d$ were blended with a normal (hydrogenous) diblock SB in such a way that the scattering-length densities of the S and B phases were matched, eliminating (inter- and intradomain) structural scattering and thus (presumably) leaving scattering from isolated $B_d$ chains as the dominant scattering mechanism.

The present study is a further attempt to use deuteriated probe molecules to gain information about the distribution of polymer chains in a diblock system with spherical morphology—this time with the added chains in the polystyrene matrix. Samples were prepared by adding deuteriated homopolystyrene ($S_d$) to a solution of poly-

† Department of Chemical Engineering.
‡ Department of Materials Science and Engineering. Present address: E. I. du Pont de Nemours and Co., Inc., Parkersburg, WV 26102.

0024-9297/88/2221-2235$01.50/0 

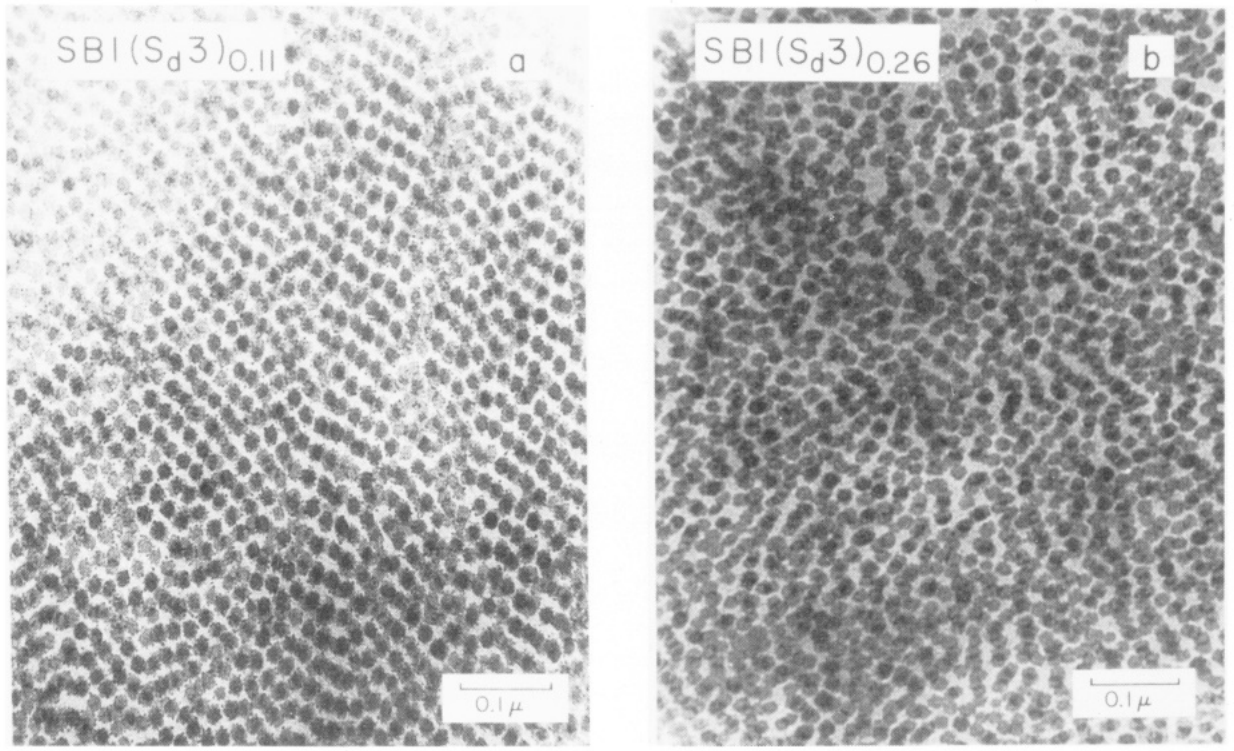


**Figure 1.** Electron micrographs of polystyrene–polybutadiene diblocks: (a) SB1 blended with 11% deuteriated polystyrene homopolymer; (b) SB1 blended with 26% deuteriated polystyrene homopolymer. Samples have been stained with $OsO_4$, which preferentially darkens the polybutadiene.

styrene–polybutadiene diblock[9] (SB1); the mixture was spin-cast and annealed to give transparent solid samples approximately 1 mm thick. These samples were then studied by using SAXS and SANS scattering.

## Experimental Section

**Materials.** The primary material used in this study was a polystyrene–polybutadiene diblock designated SB1; its synthesis and characterization are described in detail in ref 9. The number-average molecular weights of the S and B segments are 79 and 11 kdaltons, respectively, with narrow molecular weight distributions in both cases. When the material is cast from a solvent, microphase separation of the polybutadiene occurs; the B domains are roughly spherical, with an average radius[11] of 117 Å. The SANS pattern of the material[11] shows an interparticle interference peak at 0.0193 $Å^{-1}$, implying a correlation distance of 325 Å.

Deuteriated polystyrene ($S_d$) was obtained from Polysciences, Warrington, PA, in three molecular weights: 68, 196, and 385 kdaltons[12] ($Z \cong 654$, 1885, and 3702). Gel permeation chromatographic runs carried out in our laboratories gave polydispersity indices ($M_w/M_n$) of 1.07, 1.12, and 1.17, respectively, for these materials, which we shall henceforth refer to as $S_d1$, $S_d2$, and $S_d3$.

Blends of SB1 with the $S_d$ polymers were prepared by dissolving them in toluene and then forming thin films (~0.1 mm) by a solvent spin-casting technique[13] (the films were stacked and annealed to provide specimens of suitable thickness). Six samples were cast: a "dilute" series in which $S_d$ of each molecular weight was added to SB1 so that 11% of the polystyrene content was homopolymer, and a "concentrated" series in which the $S_d$ fraction was 26%.

**Structural Analysis.** Electron micrographs were obtained on a Phillips 200 electron microscope operated at 80 kV and calibrated against a diffraction grating carbon replica (21 600 lines/cm). Samples were stained with osmium tetroxide[14] and cut into sections (~400 Å thick) on an LKB ultramicrotome fitted with a freshly prepared glass knife.

Small-angle X-ray scattering (SAXS) experiments were carried out at the Rosenstiel Research Center at Brandeis University, through the courtesy of Dr. Walter C. Phillips, by using an instrument developed there.[15] Photons were supplied by an Elliott rotating-anode generator operating at 35 keV with a Cu target. The beam was focused and monochromated ($\lambda$ = 1.54 Å) by a double-mirror camera with Ni-coated mirrors. Beam size at the sample was ~0.3 × 0.4 mm. Detection of scattered X-rays was carried out by an image intensifier placed (for this experiment) 368 mm from the sample. Samples were run for 30 min each. The isotropic two-dimensional scattering patterns were then examined, corrected for detector sensitivity, and subjected to a radial average routine.

Small-angle neutron scattering (SANS) experiments were performed on the 30-m instrument at the National Center for Small-Angle Scattering Research (NCSASR), Oak Ridge National Laboratory, employing neutrons of wavelength $\lambda$ = 4.75 Å and sample-to-detector distances of 6 and 14 m. Scattering data (collected in runs of 30 min each) were corrected for background scattering and detector sensitivity and then radially averaged. Scattering intensities were reduced to absolute values by comparison with a specimen of irradiated aluminum of known $R_g$ run under the same conditions.

## Results

**Electron Microscopy.** Figure 1 shows representative micrographs of the 11% and 26% blends of $S_d3$ with SB1, designated $SB1(S_d3)_{0.11}$ and $SB1(S_d3)_{0.26}$ (compare with micrographs of unblended SB1 and $SB_d1$, Figures 1 and 2 of ref 9). The micrographs confirm that the morphology is spherical in all cases. The 11% blend is almost as well ordered as the pure SB1, but the 26% blend looks significantly different.

**SAXS Analysis.** Figure 2 shows the SAXS results for the 11% and 26% blends of $S_d1$ with SB1 (results for the $S_d2$ and $S_d3$ blends were virtually identical). The dominant features are the interparticle interference peaks around $Q$ = 0.02 $Å^{-1}$. In the 26% blends, this peak is shifted to lower $Q$, reflecting the greater separation between B domains as the amount of added homopolymer is increased. Quantitatively, the peak occurs at $Q$ = 0.0200 $Å^{-1}$ for the 11% blends (implying a correlation length $d = 2\pi/Q$ = 313 Å) and at 0.0180 $Å^{-1}$ for the 26% blends ($d$ = 350 Å).

Also apparent in the SAXS data (Figure 2) is a broad peak around 0.05 $Å^{-1}$. We attribute this to the first

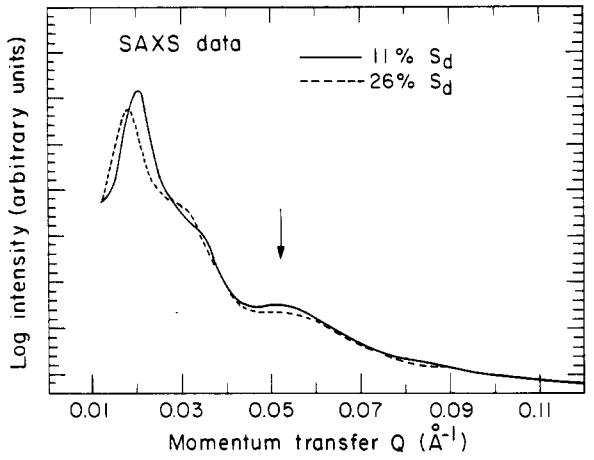


**Figure 2.** SAXS data for $SB1(S_d1)_{0.11}$ (full curve, typical of 11% samples) and $SB1(S_d1)_{0.26}$ (dashed curve, typical of 26% samples). Arrow indicates intraparticle scattering maximum from polybutadiene spheres.

maximum of the single-particle form factor[16] for the polybutadiene spheres, and we can thus calculate the average radius of these spheres as $R_B = 5.765/0.05 = 115$ Å, in close agreement with a previous estimate[11] (117 Å) for $R_B$ in SB1.

In summary, the SAXS data are sensitive to the amount of homopolystyrene added (indicated by the position of the interparticle interference maximum) but are insensitive to its molecular weight. In addition, the SAXS data for these blended samples agree with previous SANS data for unblended samples[9] in displaying a feature attributable to intraparticle scattering from spherical microdomains.

**SANS Analysis.** Figure 3a–c shows the neutron-scattering patterns obtained from the 11% blends and Figure 3d–f those from the 26% blends. The most prominent feature in these spectra is again the interparticle interference peak, located (in agreement with the SAXS data) at 0.0200 Å$^{-1}$ for the 11% blends and at 0.0180 Å$^{-1}$ for the more concentrated samples. This time, however, there are marked changes with the molecular weight of the added homopolymer $S_d$: the intensity at minimum $Q$ rises as $M_w(S_d)$ increases, and it rises faster for the 26% samples than it does for the more dilute series.

In an attempt to obtain a more quantitative understanding of the scattering in these samples, we have developed a preliminary modeling scheme for the coherent scattering that incorporates three mechanisms: (1) scattering from single chains of labeled polystyrene $S_d$, (2) interparticle interference, and (3) intraparticle scattering from the B domains. As in our studies of $SB/SB_d$ blends,[10] the single-chain scattering was modeled with a Debye function:

$$I(Q) = (2I_0/R_g^4Q^4)[R_g^2Q^2 - 1 + \exp(-R_g^2Q^2)] \quad (1)$$

where $Q$ is the magnitude of the momentum-transfer vector (equal to $4\pi\lambda^{-1}\sin\vartheta$, where $\lambda$ is the wavelength of the incident radiation and $\vartheta$ is half the scattering angle) and $R_g^2$ is the mean-square radius of gyration of the chain.

In modeling the effects of interparticle interference, we have used the treatment described by Kinning and Thomas,[17] which utilizes the closed-form solution for the Percus–Yevick[18] correlation function developed by Wertheim[19] and Thiele.[20] This solution is based on the assumption of hard-sphere behavior for the interacting particles. The calculation is parametrized mainly in terms of the hard-sphere volume fraction $\eta$:

$$\eta = \tfrac{4}{3}\pi R_{hs}^3 n \quad (2)$$

where $R_{hs}$ is the effective radius of the hard spheres and $n$ is the number of spheres per cubic centimeter. Auxiliary variables $\alpha$, $\beta$, and $\gamma$ are defined in terms of $\eta$:

$$\alpha = (1 + 2\eta)^2/(1 - \eta)^4 \quad (3)$$

$$\beta = -6\eta(1 + \eta/2)^2/(1 - \eta)^4 \quad (4)$$

$$\gamma = \tfrac{1}{2}\eta(1 + 2\eta)^2/(1 - \eta)^4 \quad (5)$$

Following Kinning and Thomas,[17] we then write the interference factor

$$S(Q,R_{hs}) = \frac{1}{1 + 24\eta(G(A)/A)} \quad (6)$$

where $A = 2QR_{hs}$ and

$$G(A) = \frac{\alpha}{A^2}(\sin A - A\cos A) + \frac{\beta}{A^3}[2A\sin A + (2 - A^2)\cos A - 2] + \frac{\gamma}{A^5}(-A^4\cos A + 4[(3A^2 - 6)\cos A + (A^3 - 6A)\sin A + 6] \quad (7)$$

Intraparticle scattering was handled as before,[9,16] with the Bessel function $J_{3/2}$ to describe the form factor:

$$f_{sphere}^2(QR_b) = \frac{9\pi}{2}\left[\frac{J_{3/2}(QR_b)}{(QR_b)^{3/2}}\right]^2 \quad (8)$$

where $R_b$ is taken as 117 Å, the radius of the B domains. Total scattering was then represented as

$$I(Q,R_{hs},R_b) = I_{chain}(Q,I_0,R_g) + KS(Q,R_{hs})\,f_{sphere}^2(QR_b) + I_{inc} \quad (9)$$

Here $I_{chain}$ is the scattering from labeled polystyrene chains $S_d$, calculated from the Debye expression (eq 1). The factor $K$ includes the contrast factor $(\rho_p - \rho_m)^2$, where $\rho_p$ and $\rho_m$ are the neutron scattering-length densities of the particle and matrix, and $I_{inc}$ is the incoherent scattering, which for these samples was constant at 0.85 cm$^{-1}$.

Given the molecular weight and isotopic composition of the labeled homopolymer chains, it is possible to calculate expected values for the forward scattering $I_0$:

$$I_0 = (a_H - a_D)^2ZN_0\phi X(1 - X) \quad (10)$$

Here $a_H$ is the sum of coherent scattering lengths[21] for the normal repeat unit, $a_D$ the corresponding sum for the deuteriated repeat unit, $Z$ the polymerization index, $N_0$ the number of repeat units per cubic centimeter in the bulk, $\phi$ the volume fraction of polystyrene in the sample, and $X$ the fraction of polystyrene that is labeled. Expected radii of gyration $R_g$ are easily calculated[22] from the expression

$$R_g = (K/\Phi)^{1/3}M_w^{1/2} \quad (11)$$

The quantity $(K/\Phi)^{1/3}$ for bulk polystyrene has been determined[23] to be 0.2. Expected values of $I_0$ and $R_g$ for the samples used in this study are listed in Table I.

Figure 3a–c shows the SANS data for the 11% samples together with the results of the calculations described above. The hard-sphere diameter $R_{hs}$, the volume fraction $\eta$, and the contrast factor $K$ were varied to secure agreement between calculation and experiment for the position and intensity of the interparticle interference peak at $Q$ = 0.02 Å$^{-1}$, and the Debye parameters $I_0$ and $R_g$ were varied to fit the points at lowest $Q$ and the general falloff of intensity as $Q$ increases. $Q$ values used in the calculations were those for which experimental points were available, and calculated spectra were run through several iterations of a Pascal seven-point smooth (in which adjacent points

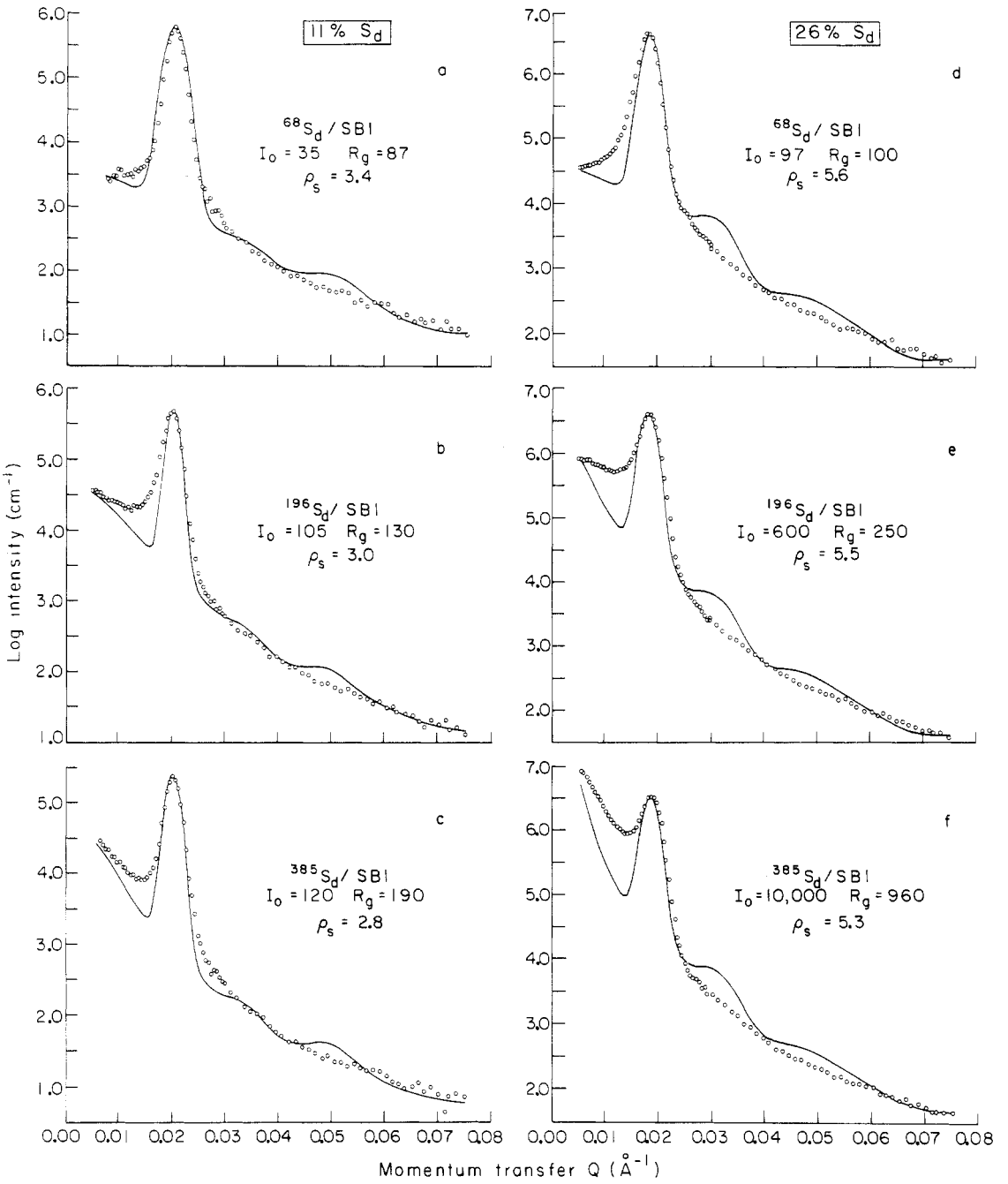


**Figure 3.** (a–c) SANS data for samples containing 11% $S_d$ in SB1; (d–f) SANS data for samples containing 26% $S_d$ in SB1. Circles represent experimental points; full lines are calculated from eq 9 by using parameters given in the figure. Molecular weight of added homopolymer $S_d$ (in kdaltons) is given as a left superscript. Scattering-length density of the polystyrene matrix as estimated from the SANS data is given as $\rho_S$.

are averaged by using the normalized coefficients of a sixth-power binomial expansion) to simulate instrumental broadening.

Inspection of Figure 3 shows that in general the algorithms used do a remarkably good job of accounting for the experiment. Two discrepancies, however, are immediately apparent. The first is that the observed interparticle interference peak is broader about the base than is the calculated peak. We take this to imply that there are ways in which the arrangement of B domains in the matrix does not correspond to a hard-sphere distribution. The second discrepancy is the complete absence in the observed spectra of the broad peak around 0.05 Å$^{-1}$ due to intraparticle scattering from the polybutadiene spheres, present in the calculated spectra and clearly seen in the SAXS data (Figure 2). We will discuss this discrepancy in more detail later.

**Table I**

| | $I_0$, cm$^{-1}$ | | | $R_g$, Å | | |
|---|---|---|---|---|---|---|
| sample | calcd | obsd | obsd/ calcd | calcd | obsd | obsd/ calcd |
| SB1($S_d1$)$_{0.11}$ | 22.9 | 35 | 1.53 | 70.4 | 87 | 1.24 |
| SB1($S_d2$)$_{0.11}$ | 66.0 | 105 | 1.59 | 119.5 | 130 | 1.09 |
| SB1($S_d3$)$_{0.11}$ | 129.6 | 120 | 0.93 | 167.5 | 190 | 1.13 |
| SB1($S_d1$)$_{0.26}$ | 47.4 | 97 | 2.0 | 70.4 | 100 | 1.42 |
| SB1($S_d2$)$_{0.26}$ | 136.6 | 600 | 4.4 | 119.5 | 250 | 2.09 |
| SB1($S_d3$)$_{0.26}$ | 268.2 | 10000 | 37.0 | 167.5 | 960 | 5.73 |

## Discussion

**Clustering of S Chains.** Values of $I_0$ and $R_g$ required to fit the observed spectra for the 11% samples (Table I) are reasonably close to the expected values, but for the 26% samples, highly inflated values of these parameters are required (Figure 4, Table I). We attribute this (as in

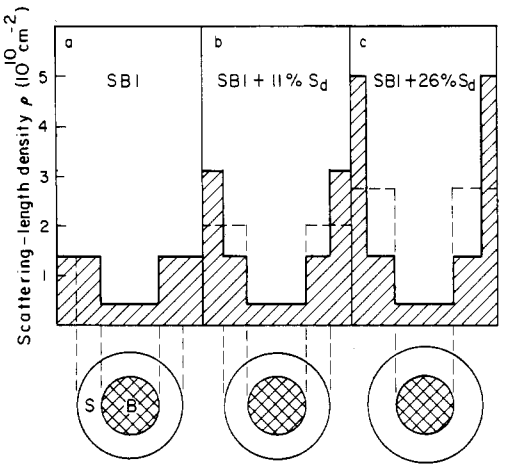


**Figure 4.** (a) SANS scattering-length density $\rho$ for SB1 in the neighborhood of a B sphere. (b) Scattering-length density for 11% added $S_d$. (c) Scattering-length density for 26% added $S_d$. In b and c, dashed lines show the $\rho$ profile if homopolymer $S_d$ is uniformly distributed throughout the matrix; the hatched area shows the $\rho$ profile if homopolymer is excluded from the corona. Estimates of $\rho_S$ support the latter conclusion.

our earlier study[10]) to clustering of the deuteriated chains, which of course would be more pronounced in the samples more concentrated in $S_d$. Note that for the 26% samples, the ratio observed/calculated for $R_g$ is close to the square root of the ratio for $I_0$, in accord with eq 10 and 11.

**Intraparticle Scattering.** In SANS experiments, the intensity of the intraparticle scattering depends on the square of the difference between the scattering-length densities of the contrasting regions. Using scattering lengths[21] for carbon and hydrogen of $0.665 \times 10^{-12}$ and $-0.374 \times 10^{-12}$ cm and densities of 1.05 g/cm$^3$ for polystyrene and 0.89 g/cm$^3$ for polybutadiene, we calculate scattering-length densities $\rho(S) = 1.414$ and $\rho(B) = 0.412$ (units are $10^{10}$ cm$^{-2}$), the difference being due to the higher C/H ratio and greater density of polystyrene. In deuteriated polystyrene ($S_d$), the substitution of deuterium (scattering length = $0.667 \times 10^{-12}$ cm) for hydrogen raises $\rho(S_d)$ to 6.47. Thus, when $S_d$ homopolymer is blended with diblock SB the scattering-length density of the polystyrene matrix is increased. This is shown graphically for a typical micelle of SB1 in Figure 4a, where scattering-length density is plotted against position with respect to the B domain (for simplicity, interfaces are represented as being sharp). In a homogeneous polystyrene blend that is 11% $S_d$, $\rho$ is raised to 1.97; if the $S_d$ content is increased to 26%, $\rho$ becomes 2.73 (dashed lines, Figure 4b,c). However, if we assume that the added $S_d$ is excluded from the corona, the interstitial regions are necessarily enriched in $S_d$. If we take the radius of the micelle (corona plus core) to be the same as the hard-sphere radius determined from the Percus–Yevick model, we can calculate that for the 11% samples ($R_B$ = 117 Å, $R_{hs}$ = 200 Å), the volume fraction of $S_d$ in the interstices is 0.337, and the corresponding $\rho$ is 3.12 (Figure 4b). For the 26% samples ($R_B$ = 117 Å, $R_{hs}$ = 215 Å), the interstitial fraction of $S_d$ is 0.705—the interstices are now mostly deuteriated—and $\rho$ = 4.98 (Figure 4c). With the known value of $\rho(B)$ given above, the values of $K$ (eq 9) required to fit the interparticle interference peak in each of the spectra can be used to deduce an apparent value of $\rho_s$. These derived values vary from 2.8 to 3.4 for the 11% $S_d$ samples and from 5.3 to 5.6 for the 26% samples (see Figure 3). The striking fact is that these "observed" values far exceed the values of $\rho_s$ calculated for a homogeneous dispersion of $S_d$ in the S matrix and are much more nearly in accord with the values of $\rho_s$ derived from the assumption that homopolymer $S_d$ is restricted to interstitial regions between the SB1 micelles (B core and S corona). An interesting additional trend is the slight reduction in $\rho_s$ as $M_w(S_d)$ is increased, perhaps due to a "fuzzing" of the boundary between coronas and interstices with increasing chain length.

We now return to the question of the missing intraparticle peaks. They were expected to appear because we implicitly assumed that the $S_d$ chains were distributed more or less evenly through the polystyrene matrix. Their absence forces us to take seriously the idea of the "hard spheres" used in the calculations described above. As has been pointed out before (see, for example, ref 4, 7, and 17), the B domains in an SB diblock are surrounded by a corona of the S segments attached to the phase-separated B segments; this corona separates the B domains and determines the effective hard-sphere radius used in the calculations.

Figure 4 demonstrates why the intraparticle scattering maximum appears in the SAXS spectra (where the B spheres are the only source of contrast, as in Figure 4a) and does not appear in the SANS data, where the S–B contrast is overshadowed by the contrast between (labeled) interstitial and coronal regions as pictured in Figure 4. This preliminary analysis assumes total exclusion of the homopolymer from the corona; a gradual depletion of homopolymer chains from regions spatially closer to the B domains is physically more reasonable. Thus, it is probable that the concept of a sigmoidal smoothing function[24] can be applied in characterizing the coronal–interstitial interface, and we intend to attempt such a characterization in a future study. Finally, we note that exclusion of added homopolymer from block copolymer micelles has been predicted in theoretical work by Whitmore and Noolandi;[7] the present study may be regarded as experimental confirmation of their predictions for the regime in which the chain length of the added homopolymer is comparable to or greater than that of the corresponding diblock material.

## Conclusions

Addition of polystyrene homopolymer to a diblock consisting of polybutadiene spheres in a polystyrene matrix increases the average separation of the B spheres in a way that may be locally anisotropic, especially with homopolymer of longer chain length.

The added homopolymer is not uniformly dispersed through the matrix but is excluded from the S corona surrounding the B spheres and is thus forced into the interstitial regions between the micelles.

**Acknowledgment.** This research has been supported by the Office of Naval Research and by the National Science Foundation, Division of Materials Research, Polymers Program, under Grant DMR-83-00446. SANS experiments were performed at the National Center for Small-Angle Scattering Research, which is funded by NSF Grant DMR-7724459 through interagency agreement 40-636-77 with the U.S. Department of Energy under Contract DE-AC05-840R21400 with Martin Marietta Energy Systems Inc. We thank Dr. George Wignall of NCSASR for his help. We also thank Dr. Walter Phillips of Brandeis University for access to his SAXS instrument and for his help in obtaining the data. Assistance with the calculations was provided by Goldy Cheng and by Peter Kofinas, with support from the MIT Undergraduate Research Opportunities Program.

**Registry No.** SBl, 106107-54-4; $S_d$, 9003-53-6; neutron, 12586-31-1.

## References and Notes

(1) Meier, D. J. *Polym. Prepr. (Am. Chem. Soc., Div. Polym. Chem.)* **1974**, *15*, 71.
(2) Helfand, E.; Wasserman, Z. *Macromolecules* **1978**, *11*, 960.
(3) Leibler, L. *Macromolecules* **1980**, *13*, 1602.
(4) Leibler, L.; Pincus, P. A. *Macromolecules* **1984**, *17*, 2922.
(5) Leibler, L.; Orland, H.; Wheeler, J. C. *J. Chem. Phys.* **1983**, *79*, 3550.
(6) Noolandi, J.; Hong, K. M. *Macromolecules* **1983**, *16*, 1443; **1982**, *15*, 482.
(7) Whitmore, M. D.; Noolandi, J. *Macromolecules* **1985**, *18*, 657.
(8) Bates, F. S.; Cohen, R. E.; Berney, C. V. *Macromolecules* **1982**, *15*, 589.
(9) Bates, F. S.; Berney, C. V.; Cohen, R. E. *Macromolecules* **1983**, *16*, 1101.
(10) Bates, F. S.; Berney, C. V.; Cohen, R. E.; Wignall, G. D. *Polymer* **1983**, *24*, 519. Berney, C. V.; Kofinas, P.; Cohen, R. E. *Polymer* **1986**, *27*, 330.
(11) Berney, C. V.; Cohen, R. E.; Bates, F. S. *Polymer* **1982**, *23*, 1222.
(12) Molecular weight values quoted were determined chromatographically.
(13) Bates, F. S.; Cohen, R. E.; Argon, A. S. *Macromolecules* **1983**, *16*, 1108.
(14) Kato, K. *Polym. Lett.* **1966**, *4*, 35.
(15) Phillips, W. C.; Rayment, I. *J. Appl. Crystallogr.* **1982**, *15*, 577.
(16) Guinier, A.; Fournet, G. *Small-Angle Scattering of X-Rays*; Wiley: New York, 1955.
(17) Kinning, D. J.; Thomas, E. L. *Macromolecules* **1984**, *17*, 1712.
(18) Percus, J. K.; Yevick, G. J. *Phys. Rev.* **1958**, *110*, 1.
(19) Wertheim, M. S. *Phys. Rev. Lett.* **1963**, *10*, 321.
(20) Thiel, E. *J. Chem. Phys.* **1963**, *39*, 474.
(21) Bacon, G. E. *Neutron Diffraction*; Oxford University Press: London, 1962.
(22) Flory, P. J. *Principles of Polymer Chemistry*; Cornell University Press: Ithaca, NY, 1953.
(23) Ballard, D.; Wignall, G. D.; Schelten, J. *Eur. Polym. J.* **1973**, *9*, 965.
(24) Hashimoto, T.; Shibayama, M.; Kawai, H. *Macromolecules* **1980**, *13*, 1237.


# Theory of the Phase Transition under Stress in Poly(butylene terephthalate)


**Radi Al-Jishi***

*Department of Physics and Astronomy, California State University, Los Angeles, Los Angeles, California 90032*

**P. L. Taylor**

*Department of Physics, Case Western Reserve University, Cleveland, Ohio 44106.*

*Received September 14, 1987; Revised Manuscript Received January 4, 1988*


ABSTRACT: Poly(butylene terephthalate) undergoes a reversible phase transition when subjected to a longitudinal stress. The temperature dependence of the critical stress is examined in terms of a model of nucleation and growth and is related to the temperature dependence of the width in stress of the hysteresis loop.


## Introduction

In a previous paper[1] two models were proposed for the reversible phase transition that occurs when poly(butylene terephthalate), PBT, is subjected to a longitudinal stress.[2-4] Both these models treated the equilibrium equation of state of PBT and were analyzed in a mean-field approximation. The principal conclusion of this work was that the width of the hysteresis in stress as the sample was cycled between $\alpha$ and $\beta$ phases was predicted to vary as $(T_c - T)^{3/2}$, with $T_c$ the critical temperature for the phase transition. This conclusion applied to both of the models examined. In the first of these, the benzene rings of the terephthalate group on one chain were bound to those on an adjacent chain by harmonic forces. In the alternative model the rings were permitted to slide past each other in a sinusoidal force field. A comparison with the work of Brereton et al.[2] showed that the hysteresis did behave in the predicted way for temperatures below $T_c$ and that the model of linked benzene rings produced a better prediction of the absolute magnitude of the hysteresis than did the other model. While it was gratifying to observe such good agreement between theory and experiment, there was some weaknesses in this treatment. One difficulty lay in the fact that the critical stress for the onset of transition was observed[3] to vary with temperature in a way not predicted in either model studied. A second inadequacy was the fact that all hysteresis was calculated to vanish sharply at $T_c$ in both models, whereas measurements found only a steady narrowing of the loop as the temperature was raised.

These discrepancies between experiment and the admittedly greatly simplified model used in ref 1 suggest a number of improvements that might be made to obtain a theory with wider predictive power. For example, the inclusion of internal degrees of freedom of the tetramethylene segment or of the terephthalate segment would add an additional temperature-dependent term to the free energy of PBT. Another likely possibility is that the boundary between the crystalline and amorphous regions of the material must be expected to contain stresses that would act to broaden the transition.

A more fundamental point, however, lies in the essentially time-dependent character of the hysteretic phenomenon. A hystersis measurement must always be performed at a frequency greater than the reciprocal of the relaxation time for the process under investigation. This raises the question of the microscopic mechanism whereby the $\alpha \rightarrow \beta$ transition takes place and necessitates a discussion of the nucleation and growth of the $\beta$ phase in a sample of $\alpha$-phase PBT.

In this paper we comment briefly on the effects of phonon frequencies and internal stresses and then describe a model for nucleation and growth in PBT.

## Phonon Frequencies

The entropy of an assembly of classical harmonic oscillators of frequencies $\omega_i$ contains the term

$$S_f = -k_B \sum_i \ln \omega_i \qquad (1)$$

In the transition from $\alpha$ to $\beta$ phase these frequencies will

0024-9297/88/2221-2240$01.50/0 